Model-Free Sliding Mode Control for a Nonlinear Teleoperation System with Actuator Dynamics

Henni Mansour Abdelwaheb, Kacimi Abderrahmane, Belaidi AEK

Abstract:

Teleoperation robotic systems control, which enables humans to perform activities in remote situations, has become an extremely challenging field in recent decades. In this paper, a Model Free Proportional-Derivative Sliding Mode Controller (MFPDSMC) is devoted to the synchronization problem of teleoperation systems subject to actuator dynamics, time-varying delay, model uncertainty, and input interaction forces. For the first time, the teleoperation model used in this study combines actuator dynamics and manipulator models into a single equation, which improves model accuracy and brings it closer to the actual system than in prior studies. Further, the proposed control approach, called Free, involves the simple measurement of inputs and outputs to enhance the system's performance without relying on any knowledge from the mathematical model. In addition, our strategy includes a Sliding Mode term with the MFPD term to increase system stability and attain excellent performance against external disturbances. Finally, using the Lyapunov function under specified conditions, asymptotic stability is established, and simulation results are compared and provided to demonstrate the efficacy of the proposed strategy.

Keywords: *Model Free Sliding Mode Controller, Teleoperation robotic systems, Actuator dynamics, Time-varying delay, Model uncertainty.*

1. Introduction

Manipulation tasks in hazardous, inaccessible, and extreme environments pose significant challenges for modern industrial technology [1–5], including space works engineering, drilling, robotic surgery, nuclear detection, undersea exploration, and even public health interventions such as physical distancing restrictions to limit the spread and transmission of the novel coronavirus [6]. Teleoperation systems are a secure solution for overcoming these challenges. Such systems are defined as the interconnection of five elements: a human operator exerting force on a local master manipulator coupled via a communication channel to a remote slave manipulator interacting with an environment to obtain a sense of telepresence via force feedback. Stability, synchronization, and transparency are the three fundamental objectives for a teleoperation system operating under numerous nonlinearities, uncertainties, and

data transmission delays. Many practical approaches have been proposed, and they can be broadly classified into model-based methods and non-model methods. Designing a model-based controller necessitates a validated mathematical model that must incorporate all of the operating circumstances of the process, which poses specific challenges for practical model-based controllers. Thus, model-based control such as computed torque control [7], inverse dynamics control [8], model reference adaptive control [9], etc., faces many obstacles in achieving the desired performance due to the presence of nonlinearities, uncertainties, transmission delays, and non-passive external interaction forces. In contrast, a non-model controller does not require prior information about the system dynamics; it adjusts online with the manipulator's unknown dynamics. That's why non-model controllers, such as the Proportional_Integral_Derivative controller (PID), are often suitable and more practical for the industrial system. However, such schemes are sensitive to parameter variations and external disturbances. They could yield poor performances when the system presents a vast operating domain. As a result, a more sophisticated and long-lasting controller is necessary to improve the performance of the nonlinear teleoperation system. Several nonlinear approaches have been developed and proposed in the literature to cope with the outcomes of the above-mentioned issues.

Z. Chen et al. developed a least square adaptive algorithm for a robust control to meet the passivity of teleoperation systems and to deal with the transparency-stability trade-off under time-varying delays [10]. A novel Barrier Lyapunov Function associated with an adaptive control algorithm is addressed for bilateral teleoperation systems to cope with output constrained issues and to achieve fixed-time convergence performance under time delays, system uncertainties and external disturbances [11]. To guarantee the system's stability, Tong et al. [12] convert the power signals of the system using wave-variable transformation. However, the system transparency performance can be largely decreased due to the issue of wave reflection [13]. The adaptive law in [14] deals with dynamic and kinematic uncertainties and ensuring the system's stability and efficient functionality, but under constant time delay. In [15], a proposed nonlinear adaptive fuzzy backstepping controller has been presented for master and slave robots to handle the nonlinearities and uncertainties. A new adaptive

neural synchronization control was presented in [16] for bilateral teleoperation systems with time-varying delay and unknown backlash-like hysteresis.

The interaction force issue between a surgical manipulator and the patient's tissues has been tackled in [17] using a nonlinear disturbance observer (DOB) with a sliding mode controller. The experimental results show the effectiveness of such a method. Utilizing a velocity observer based on a novel nonsingular fast integral terminal sliding mode (NFITSM) surface, Yana et.al. employed NFITSM based finite-time controller to cope with the synchronization problem of a teleoperation system in the presence of uncertainties [18].

Recently, a very interesting approach called Model-free control (MFC) that has been introduced by Fliess et al. [19] provides good results for practical processes.

Such an algorithm which is based on an equivalent ultra-local model of the system updated online using only input and output measurement contain normally proportional (P), proportional-integral (PI), proportional-derivative (PD), or proportional-integral-derivative (PID) controllers and compensated terms for the estimation errors. The gains of the MFC controller can be tuned through the estimations of the uncertainties, which bring out better performance compared with the classical controller. Many scholars have successfully applied the MFC scheme to deal with uncertainties and external disturbances in many areas, essentially attitude control of a quadrotor [20], a two-wheeled inverted pendulum [21], flapping-wing flying robot [22], robotic exoskeleton [23], experimental green-houses [24], glycemia regulation of type-1 diabetes [25], thermal processes [26], wheeled autonomous vehicles [27], twin-rotor aerodynamic system [28] and more. To the best of our knowledge, there is no literature on the model-free control for teleoperation systems. Furthermore, the majority of the literature cited above skipped the actuator dynamics and only considered the manipulator body dynamics. In practice, neglecting the dynamics of actuators might result in a loss of system performance or stability. For all these needs, this paper investigates a novel model-free proportional-derivative controller based on the sliding mode approach for teleoperating robotic systems, including actuator dynamics, model uncertainties, and time-varying delay. The main features of this work are as follows: first, the proposed scheme is completely model-free: that is, it only requires the measurement of inputs and outputs to improve the system's performance without depending on any information from the mathematical model. Second, compared to previous studies, the teleoperation model presented in this paper performs better in terms of accuracy and reduction of unmodeled disturbances as it incorporates more details of the actual teleoperation system by taking into account the dynamics of the actuators. Third, to overcome the implementation problem, our controller was presented as a PD controller, which is extremely useful in practice, especially for non-linear systems such as teleoperation robotics. Finally, the stability analysis of the closed-loop system is established using the Lyapunov function, and the simulation validation is presented to highlight the effectiveness of the proposed controller. The rest of the paper is structured as follows: In Section 2, which follows the introduction, the nonlinear teleoperation manipulators, including actuator dynamics, are modeled as well as properties that are involved throughout the paper. The proposed MFPDSMC controller with the stability analysis is explained in Section 3. In Section 4, simulation results are provided, followed by the conclusions in Section 5.

2. System Modeling and Problem Formulation

A master-slave teleoperation system is generally expressed in dynamic equations as follows

$$M_m(q_m)\ddot{q}_m + C_m(q_m,\dot{q}_m)\dot{q}_m + G_m = \tau_m + \tau_h$$
$$M_s(q_s)\ddot{q}_s + C_s(q_s,\dot{q}_s)\dot{q}_s + G_s = \tau_e - \tau_s$$
$$(1)$$

where $i = m, s$ stands for the master/slave manipulator, respectively; q_i, $\dot{q}_i$ and $\ddot{q}_i$ are the position, velocity, and acceleration of the master and slave dynamic systems respectively; M_i is the positive-definite inertia matrix; C_i is the matrix of centripetal and coriolis torque; G_i is the gravitational torque; τ_h and τ_e are the human-operator torque and the environment torque, respectively. τ_m and τ_s are the control input of teleoperation manipulators.

Recently, there has been a lot of interesting research into the effect of actuator dynamics on the response of manipulator robots [29]. If we consider an armature DC motor as an actuator in each joint, it can be expressed as:

$$J_{ai}\ddot{\theta}_{ai} + B_{ai}\dot{\theta}_{ai} = \tau_{ai} - g_r\tau_i \qquad (2)$$

The gear ratio g_r relating the joint position q_i and a motor shaft position θ_{ai} is described as:

$$g_r = \frac{\theta_{ai}}{q_i} \qquad (3)$$

where τ_a is the motor torque; $J_{ai} = diag(J_{a1}, J_{a2}, \ldots J_{an})$ is the moment of inertia matrix of the motor combined with the gearbox inertia and $B_{ai} = diag(B_{a1}, B_{a2}, \ldots B_{an})$ represent the viscous friction matrix of the motor shaft.

Including the actuator dynamic expression (2), the model expression (1) will be rewritten as:

$$M_{hm}\ddot{q}_m + C_{hm}\dot{q}_m + G_{hm} = \tau_{am} + g_r\tau_h$$
$$M_{hs}\ddot{q}_s + C_{hs}\dot{q}_s + G_{hs} = g_r\tau_e - \tau_{as}$$
$$(4)$$

where

$$M_{hm} = M_m g_r + J_{am} g_r^{-1}$$
$$M_{hs} = M_s g_r - J_{as} g_r^{-1}$$
$$C_{hm} = C_m g_r + B_{am} g_r^{-1}$$
$$C_{hs} = C_s g_r - B_{as} g_r^{-1}$$
$$G_{hi} = G_i g_r$$

The manipulator dynamics and the combined manipulator-motor dynamics have the following properties:

Property 1

The inertia matrix M_h is bounded and positive definite which means

$$M_h^T = M_h;$$
$$m_{\min}\|q_i\|^2 \le q_i^T M_h q_i \le m_{\max}\|q_i\|^2.$$

where $q_i \in R_{n\times 1}$ is any nonzero vector.

Property 2

The robotic manipulator is a passive system which means the matrix $\frac{1}{2}\dot{M}_h - C_h$ is skew symmetric i.e.,

$$q_i\left(\frac{1}{2}\dot{M}_h - C_h\right)\dot{q}_i = 0 \tag{5}$$

3. Controller Design

3.1. The Proposed MFPDSMC Controller

A Model-Free Control is a nonlinear control in which the mathematical model of a system is replaced by an ultra-local model equation with a small number of parameters. Those parameters are updated just by the input–output information of the system. The expression of ultra-local modelling is given by:

$$y^{(n)} = F + \alpha\tau_a \tag{6}$$

where
- y is the output of the plant.

- n is the order of time derivation of the output y (generally n is chosen equal to 1 or 2).

- F is the unknown part of all exogenous perturbations and unmodeled dynamics such as nonlinearities and uncertainties.

- τ_a is the control torque.

- α is an arbitrary constant parameter chosen such that $y^{(n)}$ and $\alpha\tau_a$ have the same size.

By taking $n = 2$. The estimate of F is defined as follows:

$$\hat{F} = \hat{y}^{(2)} - \alpha\tau_a \tag{7}$$

where $\hat{y}$ is the estimate of y.

For the estimation of y, various strategies are used based on algebraic methods [30]. To avoid the algebraic loop issues, we take a first-order derivative plus a low-pass filter to generate $\hat{y}$:

$$H = \left(\frac{K_1 s}{T_1 s + 1}\right)^2 \tag{8}$$

The MFPDSMC control law for master and slave robots can be defined as follows:

$$\tau_{am} = \left(\frac{1}{\alpha}\right)\left(-\hat{F}_m + \ddot{q}_s(t - T) - K_p e_m - K_d \dot{e}_m\right)$$
$$-(KS_m + \mu sign(S_m))$$
$$\tau_{as} = \left(\frac{1}{\alpha}\right)\left(-\hat{F}_s + \ddot{q}_m(t - T) - K_p e_s - K_d \dot{e}_s\right)$$
$$-(KS_s + \mu sign(S_s)) \tag{9}$$

where

$$e_m = q_m(t) - q_s(t - T) \tag{10}$$
$$e_s = q_s(t) - q_m(t - T) \tag{11}$$
$$S_m = \dot{e}_m - \lambda e_m \tag{12}$$
$$S_s = \dot{e}_s - \lambda e_s \tag{13}$$

$$\ddot{\hat{q}}_m(t - T) = \left(\frac{K_1 s}{T_1 s + 1}\right)^2 \ddot{q}_m(t - T)$$
$$\ddot{\hat{q}}_s(t - T) = \left(\frac{K_1 s}{T_1 s + 1}\right)^2 \ddot{q}_s(t - T) \tag{14}$$

Using Equation (7), the teleoperation system model can be rewritten as:

$$\ddot{q}_m(t) = F_m + \alpha\tau_{am}$$
$$\ddot{q}_s(t) = F_s + \alpha\tau_{as} \tag{15}$$

By making a good estimate of F, i.e., $\hat{F}_i \Rightarrow F_i$, combining Eqs. (16) and (10) yields:

$$\ddot{e}_m + K_p e_m + K_d \dot{e}_m + (KS_m + \mu sign(S_m)) = 0$$
$$\ddot{e}_s + K_p e_s + K_d \dot{e}_s + (KS_s + \mu sign(S_s)) = 0 \tag{16}$$

Note that we end up with a linear differential equation with a constant coefficient. The estimated term of F that manages the unknown part of all exogenous perturbations and unmodeled dynamics makes it simple to tune K_p and K_d for satisfactory performance. This is a substantial advantage when contrasted with the classic PD.

3.2. Stability Analysis

Define the Lyapunov function V as:

$$V = \frac{1}{2}S_m^2 + \frac{1}{2}S_s^2 \tag{17}$$

The time derivative of V is:

$$\dot{V} = S_m \dot{S}_m + S_s \dot{S}_s \tag{18}$$

Introducing a state variable error such as:

$$x_{m1} = e_m$$
$$x_{m2} = \dot{e}_m \tag{19}$$

$$x_{s1} = e_s$$
$$x_{s2} = \dot{e}_s \tag{20}$$

The sliding surfaces are rewritten using the new state variables:

$$S_m = x_{m2} + \lambda x_{m1}$$
$$S_s = x_{s2} + \lambda x_{s1} \tag{21}$$

The time derivative of S_m and S_s are:

$$\dot{S}_m = \dot{x}_{m2} + \lambda x_{m2}$$
$$\dot{S}_s = \dot{x}_{s2} + \lambda x_{s2} \tag{22}$$

Since the same procedure is used to estimate $F_i, \ddot{q}_i, \ddot{q}_m(t - T)$ and $\ddot{q}_s(t - T)$, we can define the estimation error e_{est} as:

$$e_{est\_m} = F_m - \hat{F}_m = \ddot{q}_m - \ddot{\hat{q}}_m$$
$$= \ddot{q}_s(t - T) - \ddot{\hat{q}}_s(t - T) \tag{23}$$
$$e_{est\_s} = F_s - \hat{F}_s = \ddot{q}_s - \ddot{\hat{q}}_s$$
$$= \ddot{q}_m(t - T) - \ddot{\hat{q}}_m(t - T) \tag{24}$$

Introducing (10) in (16), we get:

$$
\begin{aligned}
\ddot{q}_m &= F_m - \hat{F}_m + \ddot{q}_s(t-T) - K_p e_m \\
&\quad - K_d \dot{e}_m - \alpha(K S_m + \mu sign(S_m)) \\
\ddot{q}_s &= F_s - \hat{F}_s + \ddot{q}_m(t-T) - K_p e_s \\
&\quad - K_d \dot{e}_s - \alpha(K S_s + \mu sign(S_s))
\end{aligned}
\tag{25}
$$

We have the time derivative of x_{m2} and x_{s2} are:

$$
\begin{aligned}
\dot{x}_{m2} &= \ddot{q}_m(t) - \ddot{q}_s(t-T) \\
\dot{x}_{s2} &= \ddot{q}_s(t) - \ddot{q}_m(t-T)
\end{aligned}
\tag{26}
$$

Replacing by (26) in (25), we get:

$$
\begin{aligned}
\dot{x}_{m2} &= F_m - \hat{F}_m - (\ddot{q}_s(t-T) - \ddot{q}_s(t-T)) \\
&\quad - K_p e_m - K_d \dot{e}_m - \alpha(K S_m + \mu sign(S_m)) \\
\dot{x}_{s2} &= F_s - \hat{F}_s - (\ddot{q}_m(t-T) - \ddot{q}_m(t-T)) \\
&\quad - K_p e_s - K_d \dot{e}_s - \alpha(K S_s + \mu sign(S_s))
\end{aligned}
\tag{27}
$$

From the statements (20), (21), (24), and (25), the expression (27) follows:

$$
\begin{aligned}
\dot{x}_{m2} &= -K_p x_{m1} - K_d x_{m2} - \alpha(K S_m + \mu sign(S_m)) \\
\dot{x}_{s2} &= -K_p x_{s1} - K_d x_{s2} - \alpha(K S_s + \mu sign(S_s))
\end{aligned}
\tag{28}
$$

Considering (28), (22) can be rewritten as:

$$
\begin{aligned}
\dot{S}_m &= -K_p x_{m1} - K_d x_{m2} - \alpha(K S_m + \mu sign(S_m)) \\
&\quad + \lambda x_{m2} \\
\dot{S}_s &= -K_p x_{s1} - K_d x_{s2} - \alpha(K S_s + \mu sign(S_s)) \\
&\quad + \lambda x_{s2}
\end{aligned}
\tag{29}
$$

Using (29), $\dot{V}$ can be expressed as:

$$
\begin{aligned}
\dot{V} &= S_m[-K_p x_{m1} - K_d x_{m2} - \alpha(K S_m + \mu sign(S_m)) \\
&\quad + \lambda x_{m2}] + S_s[-K_p x_{s1} - K_d x_{s2} \\
&\quad - \alpha(K S_s + \mu sign(S_s)) + \lambda x_{s2}]
\end{aligned}
\tag{30}
$$

Two cases are considered at this stage:

Case 1: If $|S_i| \leq \gamma_i$

With $(\gamma_i > 0)$ is the boundary layer thickness of $sign(S_i)$, then:

$$
\begin{aligned}
\dot{V} \leq S_m\Big[&-K_p x_{m1} - K_d x_{m2} \\
&- \alpha K S_m + \mu \frac{S_m}{\gamma_m} + \lambda x_{m2} \Big] \\
+ S_s\Big[&-K_p x_{s1} - K_d x_{s2} - \alpha K S_s \\
&+ \mu s \frac{S_s}{\gamma_s} + \lambda x_{s2} \Big]
\end{aligned}
\tag{31}
$$

Yet

$$
\dot{V} \leq -\alpha \left[\left(K + \frac{\mu}{\gamma_m} \right) S_m^2 + \left(K + \frac{\mu}{\gamma_s} \right) S_s^2 \right]
\tag{32}
$$

with

$$
\begin{aligned}
-K_p x_{m1} - (K_d - \lambda) x_{m2} &= 0 \\
-K_p x_{s1} - (K_d - \lambda) x_{s2} &= 0
\end{aligned}
\tag{33}
$$

Equation (33) is verified if

$$
x_{i1} = e^{-(\frac{K_p}{\lambda - K_d})t}
\tag{34}
$$

To guarantee $x_{i1} \Rightarrow 0$, we must have:

$$
\frac{K_p}{\lambda - K_d} > 0
\tag{35}
$$

Consequently

$$
K_p > 0 \quad \text{and} \quad \lambda > K_d
\tag{36}
$$

For the first part of $\dot{V}$, $\dot{V} < 0$ if and only if

$$
\alpha \neq 0 \quad \text{and} \quad K > -\left(\frac{\mu}{\gamma_i} \right)
\tag{37}
$$

Case 2: If $|S_i| > \gamma_i$

$$
\begin{aligned}
\dot{V} \leq &\, S_m[-K_p x_{m1} - K_d x_{m2} - \alpha K S_m + \mu \alpha + \lambda x_{m2}] \\
&+ S_s[-K_p x_{s1} - K_d x_{s2} - \alpha K S_s + \mu s \alpha + \lambda x_{s2}]
\end{aligned}
\tag{38}
$$

Additionally

$$
\dot{V} \leq -\alpha K S_m^2 - \alpha K S_s^2
\tag{39}
$$

with

$$
\begin{aligned}
-K_p x_{m1} - K_d x_{m2} - \mu \alpha + \lambda x_{m2} &= 0 \\
-K_p x_{s1} - K_d x_{s2} - \mu \alpha + \lambda x_{s2} &= 0
\end{aligned}
\tag{40}
$$

To check Eq. (40), x_{i2} must be equal to:

$$
x_{i2} = \frac{K_p x_{i1} + \mu \alpha}{\lambda - K_d}
\tag{41}
$$

Then

$$
K_p \neq \lambda; \forall \mu, \alpha > 0; x_{i2} > \frac{K_p x_{i1} + \mu \alpha}{\lambda - K_d}
\tag{42}
$$

4. Simulation Results

In this section, simulation results are presented to validate the effectiveness of the proposed MFPDSMC controller for a teleoperation system consisting of a pair of 2-DOF haptic manipulators. The simulation was performed using Simulink and the fixed-step solver ode1 (Euler), with a sampling time of 0.001 seconds for 30 seconds. The parameters of the master-slave teleoperation system under actuator dynamics are chosen as follows:

$$
M_i = \begin{pmatrix} M_{11} & M_{12} \\ M_{21} & M_{22} \end{pmatrix}, C_i = \begin{pmatrix} C_{11} & C_{12} \\ C_{21} & C_{22} \end{pmatrix},
$$

$$
G_i = \begin{pmatrix} G_1 \\ G_2 \end{pmatrix}
$$
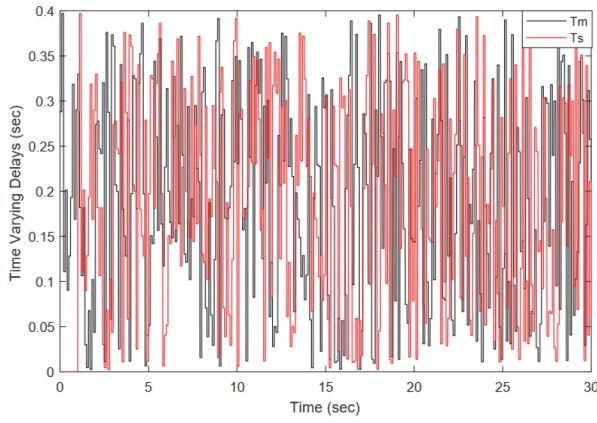
Figure 1. Forward and backward time delays

where

$$M_{11}(q) = m_1 l_{c1}^2 + m_2 l_{c2}^2 + m_2 l_1^2 + 2m_2 l_1 l_{c2}\cos(q_2)$$

$$M_{12}(q) = M_{21}(q) = m_2 l_{c2}^2 + m_2 l_1 l_{c2}\cos(q_2)$$

$$M_{22}(q) = m_2 l_{c2}^2$$

$$C_{11}(q,\dot{q}) = -m_2 l_1 l_{c2}\sin(q_2)\dot{q}_2$$

$$C_{12}(q,\dot{q}) = -m_2 l_1 l_{c2}\sin(q_2)(\dot{q}_1 + \dot{q}_2)$$

$$C_{21}(q,\dot{q}) = m_2 l_1 l_{c2}\sin(q_2)\dot{q}_1$$

$$C_{22}(q,\dot{q}) = 0$$

$$G_1 = m_2 g l_{c2}\cos(q_1 + q_2) + m_1 g l_{c1}\cos(q_1)$$
$$\qquad + m_2 g l_1 \cos(q_1)$$

$$G_1 = m_2 g l_{c2}\cos(q_1 + q_2)$$

with

$$m_1 = 3.55 \text{ Kg}; \; m_1 = 3.55 \text{ Kg}; \; l_1 = 205 \text{ mm};$$
$$l_2 = 210 \text{ mm}; \; l_{c1} = 154.8 \text{ mm}; \; l_{c2} = 105 \text{ mm};$$
$$g = 9.81 \text{ m/s}^2$$

For the actuator dynamics parameters, we have:

$$g_{r1} = 60; \; g_{r2} = 30; \; B_{a1} = g_{r1}^2 \times 2 \times 10^{-5};$$
$$B_{a2} = g_{r2}^2 \times 1.3 \times 10^{-5}$$
$$J_{a1} = g_{r1}^2 \times 3.7 \times 10^{-5}; \; J_{a2} = g_{r2}^2 \times 1.47 \times 10^{-4}$$

The forward and backward time delays in the communication channel (Tm and Ts respectively) are chosen to be random variables with an upper bound equal to 0.4 seconds (Fig. 1).

To highlight the performance of the proposed MFPDSMC controller, comparisons with the classical Proportional-Derivative controller (PD) and the Model Free Proportional-Derivative controller (MFPD) have been conducted. The PD controllers are:

$$\tau_m = K_{p1}e_m + K_{d1}\dot{e}_m$$
$$\tau_s = K_{p1}e_s + K_{d1}\dot{e}_s$$

where

$$K_{p1} = \begin{pmatrix} 14 \times 10^{-2} & 0 \\ 0 & 1 \end{pmatrix},$$

$$K_{d1} = \begin{pmatrix} 14 \times 10^{-2} & 0 \\ 0 & 2 \times 10^{-2} \end{pmatrix}$$

The MFPD controllers are as listed below:

$$\tau_{am} = \left(\frac{1}{\alpha}\right)(-\hat{F}_m + \ddot{q}_s(t-T) - K_p e_m - K_d \dot{e}_m))$$

$$\tau_{as} = \left(\frac{1}{\alpha}\right)(-\hat{F}_s + \ddot{q}_m(t-T) - K_p e_s - K_d \dot{e}_s))$$

where

$$K_{p2} = \begin{pmatrix} 15 & 0 \\ 0 & 20 \end{pmatrix}, \; K_{d2} = \begin{pmatrix} 3 & 0 \\ 0 & 2 \end{pmatrix}, \; \alpha = \begin{pmatrix} 90 \\ 100 \end{pmatrix}$$

$$\hat{F}_m = \ddot{q}_m - \alpha\hat{\tau}_{am}(t-1)$$
$$\hat{F}_s = \ddot{q}_s - \alpha\hat{\tau}_{as}(t-1)$$

The proposed MFPDSMC controllers are given as follows:

$$\tau_{am} = \left(\frac{1}{\alpha}\right)(-\hat{F}_m + \ddot{q}_s(t-T) - K_p e_m - K_d \dot{e}_m)$$
$$\qquad - (KS_m + \mu sign(S_m))$$

$$\tau_{as} = \left(\frac{1}{\alpha}\right)(-\hat{F}_s + \ddot{q}_m(t-T) - K_p e_s - K_d \dot{e}_s)$$
$$\qquad - (KS_s + \mu sign(S_s))$$

The parameters for the controller are set as:

$$K_p = \begin{pmatrix} 15 & 0 \\ 0 & 20 \end{pmatrix}, K_d = \begin{pmatrix} 3 & 0 \\ 0 & 2 \end{pmatrix}, \alpha = \begin{pmatrix} 100 \\ 100 \end{pmatrix},$$

$$\mu = \begin{pmatrix} 0.02 \\ 0.02 \end{pmatrix}, K = \begin{pmatrix} 40 \\ 4 \end{pmatrix}, \lambda = \begin{pmatrix} 4 \\ 4 \end{pmatrix}$$

The three controllers were used in two different scenarios:

Scenario 1:

In this instance, we consider the nominal parameters of the system model (4), the time-varying delay depicted in Fig. 1, and the interaction torques between the human and the master manipulator and between the remote environment and the slave manipulator as follows [31, 32] (Fig. 2):

$$\tau_h = -N_m - L_m q_m - D_m \dot{q}_m$$
$$\tau_e = N_s + L_s q_s + D_s \dot{q}_s$$

with

$$N_m = N_s = \begin{pmatrix} 1.5 \\ 1.5 \end{pmatrix}, L_m = L_s = \begin{pmatrix} 3 & 0 \\ 0 & 3 \end{pmatrix},$$

$$D_m = D_s = \begin{pmatrix} 6 & 0 \\ 0 & 6 \end{pmatrix}$$

Figures 3 through 5 depict the simulation findings for this scenario. These figures demonstrate that for all three controllers, the slave manipulator exactly imitates the master's trajectories, with negligible tracking errors. Clearly, the teleoperation system controlled by the MFPDSMC controller works more accurately, with a tracking error swing of about zero and less than 10^{-4} rad (Fig. 5.b), compared to the PD and MFPD
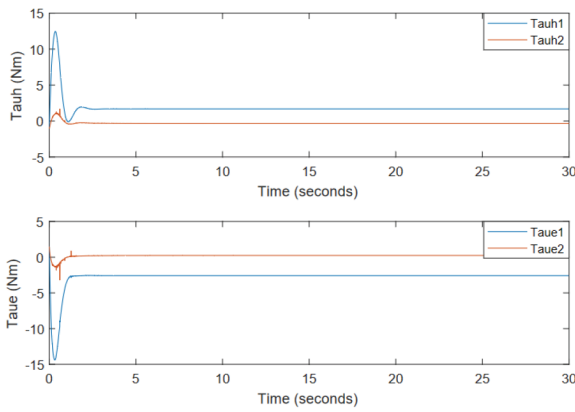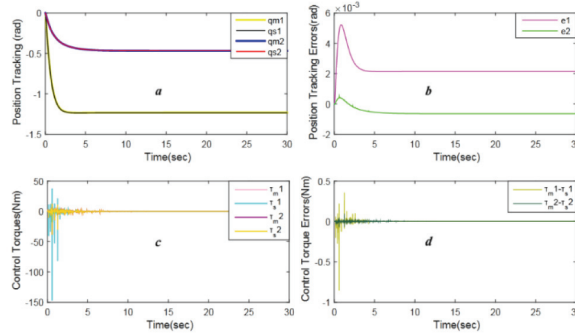
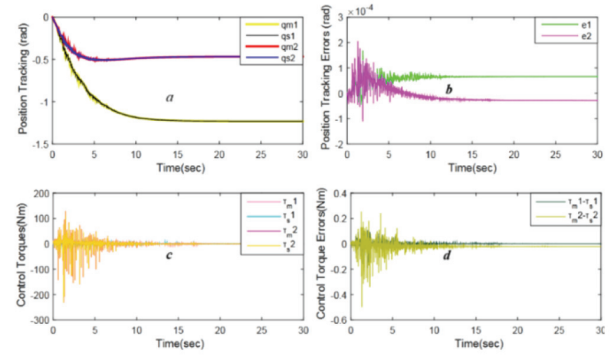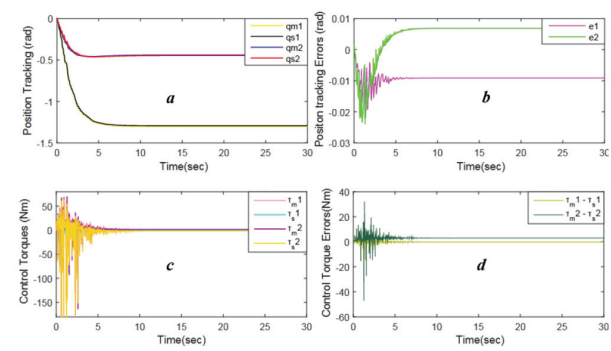**Figure 2.** The human and the environment interaction torques
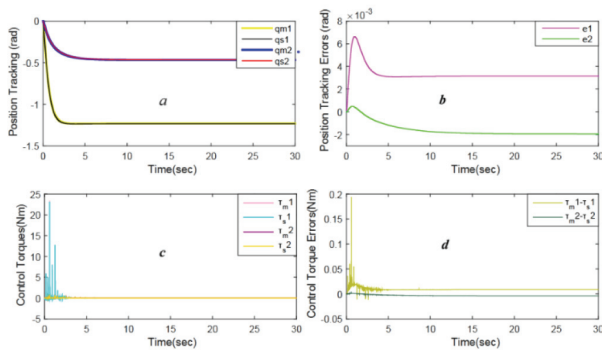
Figure 3. Simulation results with the PD controller for Scenario 1. **(a)** Position Tracking Error, **(b)** Position Tracking Error, **(c)** Control Torques and **(d)** Control Torques Errors

Figure 4. Simulation results with the MFPD controller for Scenario 1. **(a)** Position Tracking Error, **(b)** Position Tracking Error, **(c)** Control Torques and **(d)** Control Torques Errors

responses in Figs. 3.b and 4.b, where the errors reach the value of 8×10^{-3} rad.

In contrast, due to the estimation process of function F, the transient response of MFPDSMC is slightly slower (10 seconds to reach the steady-state). Figures 5(c) and 5(d) show that the master and slave control signals are very close to each other, with a maximum difference of less than 0.2 Nm. This demonstrates that the MFPDSMC approach is effective for achieving high levels of transparency.

Figure 5. Simulation results with the MFPDSMC controller for Scenario 1. **(a)** Position Tracking Error, **(b)** Position Tracking Error, **(c)** Control Torques and **(d)** Control Torques Errors

Figure 6. Simulation results with the PD controller for Scenario 2. **(a)** Position Tracking Error, **(b)** Position Tracking Error, **(c)** Control Torques and **(d)** Control Torques Errors
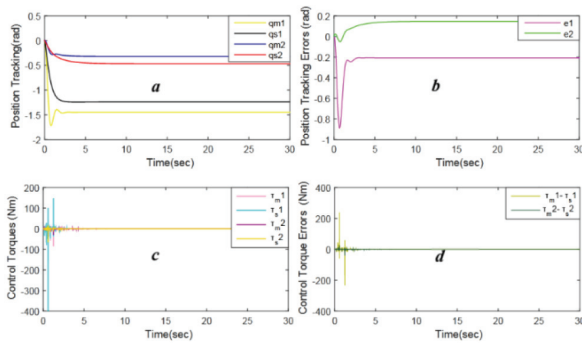
Scenario 2:

To show how well the proposed MFPDSMC controller can deal with changes in parameters and disturbances, the same conditions as the last scenario are looked at with the following uncertainties in the actuator parameters:

$$g_{r1} = 70; g_{r2} = 40; B_{a1} = g_{r1}^2 \times 3 \times 10^{-5};$$
$$B_{a2} = g_{r2}^2 \times 10^{-5}$$
$$J_{a1} = g_{r1}^2 \times 2.7 \times 10^{-5}; J_{a2} = g_{r2}^2 \times 3.47 \times 10^{-4}$$

Figures 6(a) and 7(a) demonstrate the advantages of the MFPD controller over the classical PD in terms of robustness and performance, where the elimination of the uncertain part of the system by the function F provides a straightforward tuning for the MFPD gains. Then, Figure 9 verifies the stability of the closed loop when the MFPDSMC surface values approach zero, i.e., $Si = 0$ at about $t = 4.8$ seconds with $i = m, s$. In addition, Fig. 8.c shows the MFPDSMC control signals, which appear reasonable for the closed-loop system, and Fig. 8.d illustrates that the force feedback errors are fairly modest. Therefore, even though the model parameters are not close to their values, the slave can greatly track the master, and the human operator will receive precise force feedback. This result validates the effectiveness of our control design.

Figure 7. Simulation results with the MFPD controller for Scenario 2. **(a)** Position Tracking Error, **(b)** Position Tracking Error, **(c)** Control Torques and **(d)** Control Torques Errors
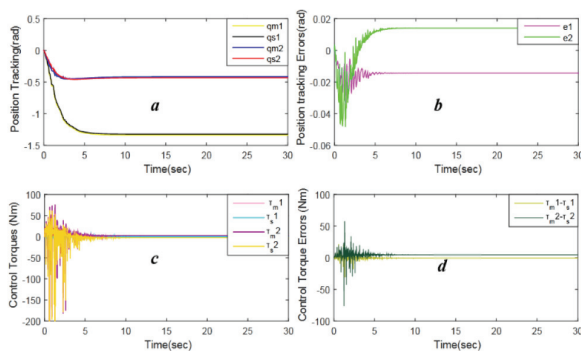
Figure 8. Simulation results with the MFPDSMC controller for Scenario 2. **(a)** Position Tracking Error, **(b)** Position Tracking Error, **(c)** Control Torques and **(d)** Control Torques Errors
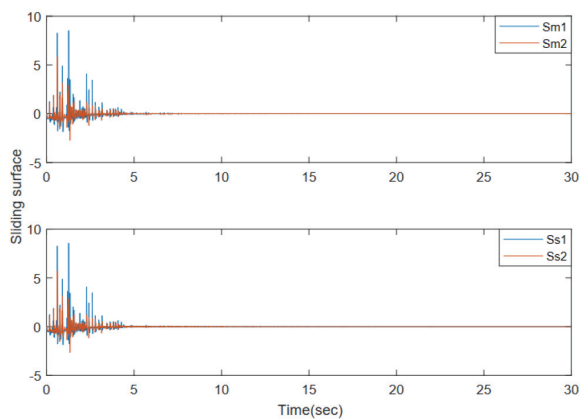
Figure 9. The values of sliding mode surface at master and slave sides

5. Conclusion

In this paper, a model-free proportional-derivative sliding mode controller has been proposed for a nonlinear teleoperation robotics system considering actuator dynamics, time-varying delays, and various uncertainties. The main feature of this work is that the derivation of the control laws does not require any knowledge of the system model since the parameter change was managed by automatically updating the control laws. Also, the high performance against external disturbances was guaranteed by the sliding mode term, which drives the system states towards the sliding surface and, eventually, to equilibrium. Furthermore, by combining the existing teleoperation model with the actuator dynamics, the teleoperation model described in this work is more challenging and performs better in terms of accuracy and reduction of unmodeled disturbance. Finally, the simulation results demonstrate the effectiveness of the proposed controller in achieving stability and transparency simultaneously and they verify the theory behind the controller design.

AUTHORS

Henni Mansour Abdelwaheb[*] – Laboratory of Automation and Systems Analysis (LAAS), National Polytechnic School of Oran Algeria, e-mail: abdelwahebhenni@gmail.com.

Kacimi Abderrahmane – Institute of Industrial Security Maintenance of Oran, Algeria, e-mail: kdjoujou@yahoo.fr.

Belaidi AEK – Laboratory of Automation and Systems Analysis (LAAS), National Polytechnic School of Oran Algeria, e-mail: belaidiaek@gmail.com.

[*]Corresponding author

References

[1] K. A. Manocha, N. Pernalete, R. V. Dubey. "Variable position mapping-based assistance in teleoperation for nuclear clean up", In: Proceedings of the 2001 ICRA IEEE International Conference on Robotics and Automation, pp. 374–379, (2001). doi: 10.1109/ROBOT.2001.932580.

[2] L. F. Penin, K. Matsumoto, and S. Wakabayashi. "Force reflection for time-delayed teleoperation of space robots", In: Proceedings of ICRA'00 IEEE International Conference on Robotics and Automation, pp. 3120–3125, (2000). doi: 10.1109/ROBOT.2000.845143

[3] R. J. Anderson, M. W. Spong. "Bilateral control of teleoperators with time delay". Proceedings of the 1988 IEEE International Conference on Systems, Man, and Cybernetics, Beijing, China, pp. 131–138, (1988). doi: 10.1109/ICSMC.1988.754257.

[4] P. F. Hokayem, M. W. Spong. "Bilateral teleoperation: an historical survey". Automatica, 42(12), 2035-2057, (2006). doi: 10.1016/j.automatica.2006.06.027.

[5] I. G. Polushin, P. X. Liu, and C. H. Lung. "A force-reflection algorithm for improved transparency in bilateral teleoperation with communication

delay", IEEE/ASME Trans. Mechatronics 12: 3, pp. 361–374, Jun. 2007.

[6] G. Yang, H. Lv, Z. Zhang et al. "Keep healthcare workers safe: Application of teleoperated robot in isolation ward for COVID-19 prevention and control". Chin. J. Mech. Eng: 33, 47, (2020). doi: 10.1186/s10033-020-00464-0.

[7] T. Abut and S. Soyguder. "Real-time control of bilateral teleoperation system with adaptive computed torque method", Industrial Robot 44: 3, pp. 299–311, (2017). doi: 10.1108/IR-09-2016-0245.

[8] X. Liu and M. Tavakoli. "Inverse dynamics-based adaptive control of nonlinear bilateral teleoperation systems" 2011 IEEE International Conference on Robotics and Automation, Shanghai International Conference Center, Shanghai, China, (2011).

[9] K. Hosseini-Suny et al. "Model reference adaptive control design for a teleoperation system with output prediction", Journal of Intelligent & Robotic Systems, 59, 319–339, (2010).

[10] Z. Chen, Y. Pan, J. Gu. "A novel adaptive robust control architecture for bilateral teleoperation systems under time-varying delays", International Journal of Robust and Nonlinear Control, 25: 17, pp. 3349–3366, (2015).

[11] Z. Wang, Y. Sun, B. Lianga. "Synchronization control for bilateral teleoperation system with position error constraints: A fixed-time approach", ISA Transactions 93, pp. 125–136, (2019).

[12] M. Tong, Y. Pan, Z. Li, and W. Lin. "Valid data based normalized crosscorrelation (VDNCC) for topography identification", Neurocomputing, 308, pp. 184–193, (2018).

[13] X. Yang, C.-C. Hua, J. Yan, and X.-P. Guan. "A new master-slave torque design for teleoperation system by T-S fuzzy approach", IEEE Transactions on Control Systems Technology, 23(4), 1611–1619, (2014).

[14] Y.-C. Liu and M.-H. Khong. "Adaptive control for nonlinear teleoperators with uncertain kinematics and dynamics", IEEE/ASME Transactions on Mechatronics 20: 5, pp. 2550–2562, (2015).

[15] Z. Chen, F. Huang, C. Yang and B. Yao. "Adaptive fuzzy backstepping control for stable nonlinear bilateral teleoperation manipulators with enhanced transparency performance", IEEE Transactions on Industrial Electronics 67: 1, pp. 746–756, (2020), doi: 10.1109/TIE.2019.2898587.

[16] H. Wang, P. X. Liu and S. Liu. "Adaptive neural synchronization control for bilateral teleoperation systems with time delay and backlash-like hysteresis", IEEE Transactions on Cybernetics 47: 10, pp. 3018-3026, (2017), doi: 10.1109/TCYB.2016.2644656.

[17] S. Hao, L. Hu and P. X. Liu. "Sliding mode control for a surgical teleoperation system via a disturbance observer", IEEE Access, 7, pp. 43383–43393, (2019), doi: 10.1109/ACCESS.2019.290 1899.

[18] Y. Yang, C. Hua, J. Li, X. Guan. "Finite-time output-feedback synchronization control for bilateral teleoperation system via neural networks", Information Sciences. 406–407. 216-233, (2017). doi: 10.1016/j.ins.2017.04.034.

[19] M. Fliess, C. Join, M. Mboup, H. Sira-Ramirez. "Vers une commande multivariable sans modele", arXiv preprint math/0603155, (2006).

[20] H. Wang, X. Ye, Y. Tian, N. Christov. "Attitude control of a quadrotor using model free based sliding model controller", In: Proc. 2015 20th International Conference on Control Systems and Science, Bucharest, Romania, pp. 149–154, (2015).

[21] C. Y. Yu, J. L. Wu. "Intelligent PID control for two-wheeled inverted pendulums", IEEE International Conference on System Science and Engineering, pp. 1–4, (2016).

[22] A. N. Chand, M. Kawanishi and T. Narikiyo. "Nonlinear model-free control of flapping wing flying robot using iPID", IEEE International Conference on Robotics and Automation, pp. 16–21, (2016).

[23] X. Wang, X. Li, J. Wang, X. Fang, X. Zhu. "Data-driven model-free adaptive sliding mode control for the multi degree-of-freedom robotic exoskeleton", Information Sciences. 327, 246–257, (2016).

[24] F. Lafont, J. Balmat, N. Passel, M. Fliess. "A model-free control strategy for an experimental green house with an application to fault accommodation", Computers and Electronics in Agriculture, 110, 139–149, (2015).

[25] T. M. Ridha and C. H. Moog. "Model free control of type-1 diabetes: A fasting-phase study", IFAC-PapersOnLine. 48:20, pp. 76–81, (2015).

[26] F. J. Carrillo, F. Rotella. "Some contributions to estimation for mode-free control", Proceedings of the 17th IFAC Symposium on System Identification, Beijing, China, pp. 19–21, (2015).

[27] B. Andrea-Novel, L. Menhour, M. Fliess, H. Mounier. "Some remarks on wheeled autonomous vehicles and the evolution of their control design", IFAC-PapersOnLine, 49(15), 199–204. (2016).

[28] R. C. Roman, M. B. Radac, R. E. Precup, E. M. Petriu. "Data-driven optimal model-free control of twin rotor aerodynamic systems", IEEE International Conference on Industrial Technology (ICIT) (pp. 161–166), Seville, Spain, (2015).

[29] N. Adhikary, C. Mahanta. "Sliding mode control of position commanded robot manipulators". Control Engineering Practice, 81, 183–198, (2018).

[30] T. Kara, A. H. Mary. "Adaptive PD-SMC for nonlinear robotic manipulator tracking control", Studies in Informatics and Control, 26(1), 49–58, (2017). doi: 10.24846/v26i1y201706.

[31] C. Hua, P. X. Liu, H. Wang. "Convergence analysis of teleoperation systems with unsymmetric time-varying delays", IEEE International Workshop on Haptic Audio Visual Environments and Games (pp. 65–69), (2008).

[32] C. C. Hua, X. P. Liu. "Delay-dependent stability criteria of teleoperation systems with asymmetric time-varying delays", IEEE Transactions on Robotics, 26(5), 925–932, (2010).